

Cross Section for $C^{12}(\alpha, \alpha n)C^{11}$ at 920 MeV*

Jonathan Radin

New York University, Bronx, New York 10453

(Received 30 October 1969; revised manuscript received 21 May 1970)

Plastic scintillators were exposed in the external 920-MeV α -particle beam at the 184-in. cyclotron at Lawrence Radiation Laboratory. The beam-flux monitor was Ilford 100- μ L4 pellicles. The cross section for $C^{12}(\alpha, \alpha n)C^{11}$ was found to be 49.4 ± 1.8 mb.

INTRODUCTION

Recent investigations of high-energy (>100 -MeV/ N)¹ cosmic rays have disclosed a need for spallation cross sections of nuclei in this energy range with protons and α particles. The interactions occur both in interstellar space where high-energy nucleons collide with the interstellar gas ($\sim 90\%$ hydrogen and $\sim 10\%$ helium),¹ and in the earth's atmosphere where the cosmic rays ($\sim 85\%$ p and $\sim 15\%$ α)² collide with the atmospheric oxygen and nitrogen. Of particular interest in the spallation reactions in interstellar space are those of the M group (C, N, O) into the L group (Li, Be, B). Cross-section measurements for the $\alpha + M$ group at $E_\alpha > 100$ MeV/ N are nonexistent. However, there are several indications that the spallation cross sections for the $\alpha + M$ group are on the average twice that for protons: (1) Alexander and Yekutieli,³ using an independent-particle optical-potential model, predict the reaction cross section for $\alpha + C$ to be more than twice that for $p + C$. (2) Jain, Lohrmann, and Teucher,⁴ examining cosmic-ray α -particle interactions ($E > 7$ GeV/ N) in emulsion, find ~ 2 nucleons of the α particle taking part in each collision. (3) $\sigma[C^{12}(x, xn)C^{11}]$, at 380 MeV, for $x = \alpha$ is approximately twice that for $x = p$.^{5,6} (4) Korteling and Hyde,⁷ examining the cross sections for $x + Nb^{93}$ reactions yielding many products with $A > 67$, with $x = p$ and $x = \alpha$ at $E_\alpha = 320$ – 720 MeV, find the cross section for α to be approximately twice that for p .

If the above implications hold, then the interstellar helium will produce $\sim 20\%$ of the spallation products in interstellar space, and the cosmic-ray α particles will produce $\sim 30\%$ of the primary spallation products in the atmosphere. It was decided to determine some of these $M(\alpha,)L$ cross sections, and I present here the $C^{12}(\alpha, \alpha n)C^{11}$ cross section, itself one of the $M(\alpha,)L$ reactions, which will also serve as a beam-monitor reaction for future experiments.

EXPERIMENTAL ARRANGEMENT

The experiment was performed with the external

920-MeV α -particle beam (see Appendix) in the medical cave of the 184-in. cyclotron at Lawrence Radiation Laboratory (LRL). A modification of a technique, developed by Cumming and Hoffman⁸ and later by Poskanzer,⁹ was employed. The target was a plastic scintillator (Pilot B),¹⁰ and the flux monitor was an Ilford 100- μ L4 pellicle¹¹ exposed perpendicular to the beam. The scintillator is an almost pure hydrocarbon, by weight 91.5% carbon and $\leq 0.5\%$ nonhydrocarbon. The percentage of carbon is based, as is customary, on the total carbon ($C^{12} + C^{13}$) content. The number is derived from the formula C_9H_{10} for the matrix material¹² of Pilot B and from chemical analysis.⁸ Both methods agree to 0.2%.

All scintillators were 3.81 cm diam by 0.32, 2.5, or 5.1 cm thick. The C^{11} gas loss from the target for α -particle bombardment was taken to be the same as for proton bombardment. There should be negligible C^{11} gas loss from all of the scintillators.¹³

Five different target arrangements were used (Fig. 1). To reduce the contribution of neutrons in the beam, the target was set up 5 m from the beam portal with a helium bag (5-mil polyethylene end windows) occupying 4 m of that space. The target was 5 m ($\sim 23^\circ$) from the undeflected beam.

Position (a) was the arrangement for the primary cross-section determination; positions (b)–(e) for secondary effects. In position (a) the target was prepared by attaching the scintillator to the pellicle with double-sided Scotch tape. The outline of the scintillator was traced on the pellicle with a pencil to locate the scintillator position after development of the pellicle. The pellicle-scintillator sandwich was wrapped light tight in black paper and mounted on 2-mil stretched Mylar. The exposures were for 7 sec, and the counting was begun about 9.5 min later. Initial count rates were ~ 1000 counts/min.

Positions (b) and (c) were to determine the correction to an infinitely thin target. The 12.5 cm separating the upstream from the downstream scintillator served to reduce the solid angle exposed by one scintillator to the isotropic secondaries from the other. Both downstream scintillators are in the same beam environment and can be confidently

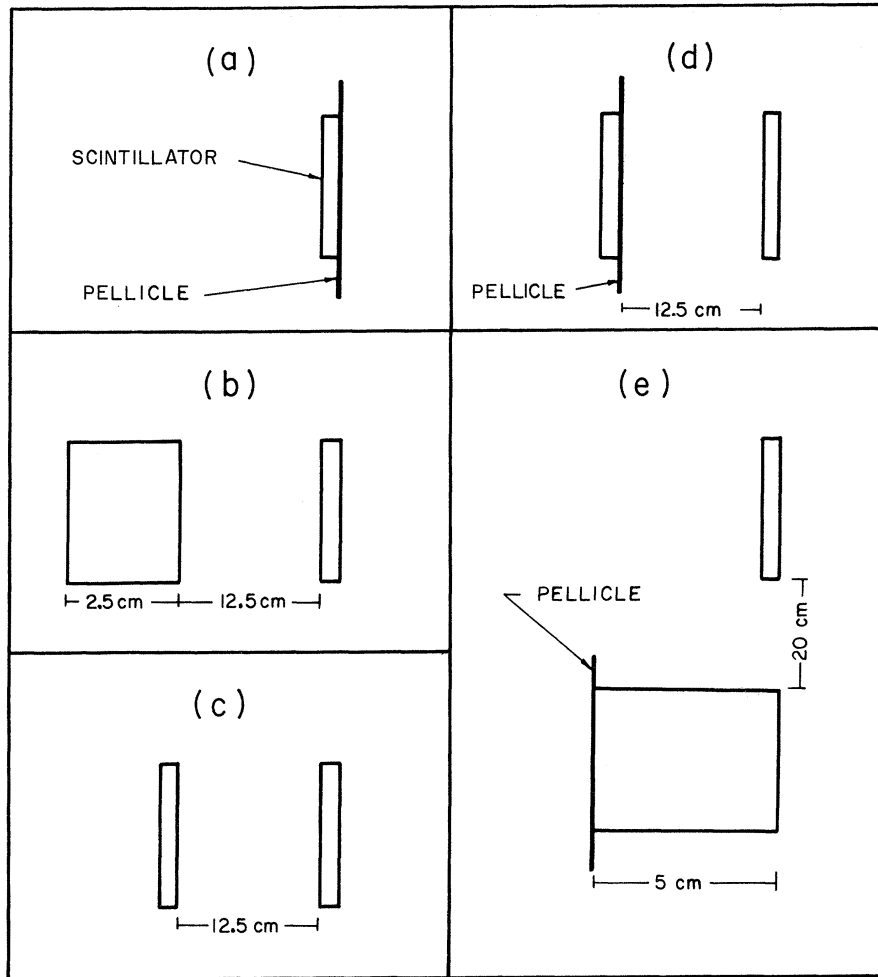


FIG. 1. Target arrangements. The α -particle beam is incident from the right. (a) Primary cross section determination. (b)–(e) Secondary effects.

compared. Two unknowns were assumed: (1) constant beam scatter by the upstream scintillator, (2) defining $\Sigma_{C^{11}}^{rel}(x)$ as the relative cross section for C^{11} production in a target x cm thick to a target of zero thickness, then $\Sigma_{C^{11}}^{rel}(x) = ax$. Normalizing on the upstream scintillator and intercomparing the downstream scintillators, the coefficient a was found to be $(0.26 \pm 0.10)\%$ per 100-mg/cm^2 polystyrene. The correction for the 0.32-cm -thick scintillator was $(0.8 \pm 0.4)\%$.

The contribution of the pellicle to the C^{11} produced was estimated from the $\Sigma_{C^{11}}^{rel}(x)$ found above. Assuming that (1) the coefficient a is independent of atomic weight, and (2) the ratio of the effect of external to internal secondaries is 2, the pellicle contribution was estimated to be $(0.2 \pm 0.2)\%$. In target arrangements (c) and (d), by normalizing on the upstream scintillators and intercomparing the downstream scintillators, the effect of the pellicle was verified to be $<2\%$.

Arrangement (e) was to determine the contribu-

tion of neutrons in the beam to the C^{11} production. Here a 0.32-cm scintillator was exposed on beam center, and a 5.1-cm scintillator and emulsion were exposed 20 cm off beam center (see Appendix); the assumption was made that the neutrons were unfocused. The neutron contamination was negligible.

To determine the deuteron contamination of the beam a $200\text{-}\mu$ G5 or a $200\text{-}\mu$ Kodak NKG emulsion was exposed for flat tracks prior to the first and eighth runs. The deuterons are $2I_{\min}$ and the α particles are $8I_{\min}$ (I_{\min} is the minimum ionization-energy-loss rate of a singly charged particle), and their tracks are easily separable without resort to grain counting. No deuterons had been run for four months prior to the runs in position (a), and the deuteron contamination was $<(0.5 \pm 0.5)\%$ and not included in the corrections.

MEASUREMENTS

Target counting. The scintillation detection

equipment was located in the concrete-shielded cave of the Health Physics group at LRL. In addition, to further reduce background, the photomultipliers were surrounded by 5 cm of low-activity lead bricks with an inner shield of 0.32-cm iron to absorb the lead x rays. The background in the 0.32-cm scintillators was 13–15 counts/min, constant within 3% for each photomultiplier, varying only from one photomultiplier to another.

On each photomultiplier (Amperex 56DVP or RCA 8575) was epoxied a Lucite light pipe shaped as a right circular cylinder 4.19 cm diam by 0.32 cm thick. A thin disk 3.94 cm by 0.08 cm centered on the top surface of the Lucite was removed; the cavity served to center the scintillator. The light pipe separated the scintillator from possible radioactivity in the photomultiplier glass (e.g., K^{40}) which would contribute to the background, but primarily served as a scintillator holder. No reduction in background was observed in the use of these light pipes.

After exposure, the scintillator was detached from the emulsion and wiped by a moist Kimwipe to reduce static charge and possible 30-min-half-life effects⁸ (although this was never observed here). The scintillator was optically coupled with mineral oil to the light pipe and wrapped with two layers of Al foil, diffuse face down. The problem of photocathode relaxation after white-light exposure was overcome by taking advantage of the S11 response of these photocathodes. The S11 response is down two orders of magnitude in the red region ($\lambda > 6200 \text{ \AA}$)¹⁴ The mounting operation was performed in red light via a Kodak $5\frac{1}{2}$ -in. safe-light filter 1A with a 10-W bulb at about 1 m.

Photomultiplier stability after this mounting technique was such that peak (Am^{241} 60 keV) drifts were <2% from 10 sec after voltage was applied to the photomultiplier to over 5 h later. The whole system of preamplifier, amplifier, discriminator, and scaler was stable to $\pm 1\%$ variation over both short-time (minutes) fluctuations and long-time (days) drifts.

After mounting the scintillator, an Am^{241} source was placed on the scintillator, and the 60-keV photopeak was observed with a 100-channel analyzer. The peak was then reaccumulated in anticoincidence with the output of a threshold discriminator (connected in parallel with the analyzer to the output of the amplifier). The threshold was adjusted until the anticoincidence edge was on the 60-keV photopeak. The output of the discriminator was connected to a scaler, and all disintegrations giving rise to pulses greater than 60 keV were counted. The scintillator was counted for ≥ 3 half-lives with counts recorded at 2-min intervals. At this time the relative light collection efficiency of

the scintillator and photomultiplier was determined by a mapping of the scintillator with a collimated Am^{241} source, tabulating pulse height versus source position. Correction was made to the counting efficiency using the efficiency curve of Cumming⁸ at 60-keV discriminator threshold, and efficiencies of $(94.0 \pm 0.5)\%$ ^{8,15} for the 0.32-cm scintillator and $(97.0 \pm 0.5)\%$ for the 2.5-cm scintillator were used. The Cumming efficiency curve was constructed on the assumption that the light emission from the scintillator was a linear function of electron energy deposition from 0 to 622 keV. No correction was added here for the nonlinearity below 100 keV. Background in the scintillators was determined before and well after exposure. The change was negligible.

The integral counts to each 2-min interval were least-squares fitted to a decaying exponential (20.35-min half-life)¹⁶ plus constant background to determine the amount of C^{11} at the end of the exposure.¹⁷ The decay of C^{11} during the 7-sec irradiation amounted to 0.4% and was corrected. The background was both fitted to and supplied. The fitted background agreed to within 20% with the empirically observed background, and the resulting differences in the initial quantity of C^{11} between the two calculations amounted to $(0.5 \pm 0.3)\%$. Since the background was very reproducible, the observed-background solution was used. The $\chi^2/(\text{degree of freedom})$ for the curves were $\lesssim 0.3$,¹⁸ except for two runs during which there was independent evidence that the apparatus was malfunctioning. These runs were not included in the calculations.

As a search for a short-half-life particle [10-min N^{13} from $C^{12}(\alpha, T)N^{13}$ and $C^{13}(\alpha, p3n)N^{13}$ charge exchange, or miscellaneous effects such as photomultiplier relaxation or C^{11} gas loss from the target], two higher-intensity runs differing by a factor of 10 in beam intensity were made. The analysis was carried out with a program LSQVMT¹⁹ which minimizes the χ^2 by an iterative gradient with a variable-metric algorithm. The two runs were intercompared when the count rate of the more heavily exposed target was the same as the initial count rate of the lesser exposed target. In the higher-intensity exposure the shorter half-lives would have decayed. Both decay curves gave $\sim 1\%$ contamination, with a contaminant half-life of ~ 10 min. No significant change in the half-life or % contamination was observed between the two runs. Since the data accumulation method (visual readout) was considered accurate to only three significant figures, the above numbers are not considered significant, and no correction was made to the C^{11} results for contamination except to include an additional uncertainty of 1% in the amount of C^{11} created. The heavily exposed scintillator was also

used to determine the apparatus dead time.

Pellicle. Three types of emulsion were considered and tested for monitoring, 100- μ Ilford G5, L4, and K2.¹¹ The L4 was chosen over the G5 for two reasons. First, the developed Ag cross-section area of the plunging tracks was smaller by about a factor of 2 (~ 0.65 - μ diam for the L4 compared to ~ 1 - μ diam for the G5) for the $8I_{\min}$ α particles. This permitted higher fluxes by a factor of 2 for the L4. Second, the G5 accumulated electron tracks from the background. The L4, although supposedly equally sensitive to these minimum ionizing tracks, did not accumulate background. The K2 was similar to the L4 in its $8I_{\min}$ track cross-section area and in being free of background. The L4 was chosen over the K2 because of the listed greater sensitivity of the L4,²⁰ although this was not tested here. The possibility of deuteron contamination in the cyclotron ($2I_{\min}$) was an argument for the use of L4.

The L4 was able to retain distinct tracks with local fluxes of 1×10^7 α /cm². Above this number the tracks overlapped and intertrack areas were gray—perhaps from scattered light or spontaneously developed grains. In target exposures, peak local fluxes of 1.5×10^7 /cm² were encountered and average fluxes were 4 – 6×10^6 /cm², an increase by over a factor of 2 from previous use.

A dead-space correction assuming nonseparation of two tracks when the track centers were one track radius apart produced, typically, an expected 3% loss of tracks at local fluxes of 1×10^7 . The dead-space correction was performed on each 100- μ^2 area counted on each plate. The scanning efficiency was checked by independent rescanning by a second scanner, and agreement was $100 \pm 2\%$.

The pellicles were mounted using the "Heckman method"²¹ and developed for 20 min in D-19 diluted 1:6 at $(21 \pm 2)^\circ\text{C}$. More than about 5000 tracks pellicle were counted in a 19-point scan pattern centered in the etched outline of the scintillator. In one case ~ 9000 tracks were counted. The scanning microscope contained a 100 \times objective and a 25 \times ocular. A special 36-box grid reticle was cut for the microscope at LRL. The reticle area was calibrated on the microscope to 1% accuracy.

The flux at the 19 points was fitted to an area function in two ways: first, by a linear least-squares fit to a six-parameter area function¹⁷; second, to a six-parameter product of a quadratic in x and y . The coefficients in the latter case were determined by LSQVMT.¹⁹ Both procedures agreed to 1%. The ratio of flux contribution from higher-order terms to the uniform-flux term was 4–8%, attesting to the uniformity of the beam. In addition, as a check on the above calculation, the flux was averaged over the 19 points and, assuming a uniform beam, the flux so determined agreed to within 2% with the area-fitted flux. The flux uncertainty was taken as

$$\left[\sum_{i=1}^6 \left(\Delta a_i \frac{\partial F}{\partial a_i} \right)^2 \times \frac{\chi^2}{(\text{degree of freedom})} \right]^{1/2},$$

where F is the analytic expression for the integrated flux, and the a_i are the six parameters. The resulting uncertainties are tabulated in Table I.

There were seven runs in position (a) with instrument or human failure in five runs. In Table I are tabulated the data, corrections, and error estimates for the two good runs. The random errors

TABLE I. Corrections and error estimates.

Effect (units-error type ^a)	Run 5	Run 7
C ¹¹ in target at end of exposure (atoms-R)	4.17×10^4 ($\pm 1\%$)	4.19×10^4 ($\pm 1\%$)
Target weight (g -R)	3.74 ($\pm 0.5\%$)	4.575 ($\pm 0.5\%$)
Number of tracks counted	8896	5850
Flux through scintillator (R)	55.7×10^6 ($\pm 2.8\%$)	46.0×10^6 ($\pm 5\%$)
Reticle calibration (S)	$\pm 1\%$	$\pm 1\%$
Scanning efficiency (R, S) ^b	$\pm 1\%, \pm 1\%$	$\pm 1\%, \pm 1\%$
Scintillator position (R)	$\pm 0.5\%$	$\pm 0.5\%$
Pellicle stretching (S)	$\pm 1\%$	$\pm 1\%$
Extrapolation to thin target (S)	$(0.86 \pm 0.4)\%$	$(1.06 \pm 0.5)\%$
Contribution of pellicle to C ¹¹ (S)	$(0.2 \pm 0.2)\%$	$(0.2 \pm 0.2)\%$
Track overlap in pellicle (R)	$(0.2 \pm 0.2)\%$	$(0.1 \pm 0.1)\%$
Nonuniformity of photocathode (R)	$(0.3 \pm 0.3)\%$	0.0%
C ¹² ($\alpha, \alpha n$)C ¹¹	49.4 mb	49.3 mb
rms errors (R)	3.5%	5.4%
rms errors (S)	2.1%	2.1%

^aR = random, S = systematic.

^bThe scanning uncertainty of 2% was separated into 1% R and 1% S.

TABLE II. Cross sections for C^{11} production in α and p irradiations. Errors are $\sim 5\%$ in cross sections and $\sim 7\%$ in ratios.

E_α (MeV)	$\sigma_\alpha(E_\alpha)$ (mb)	$\sigma_p(E_\alpha)$ (mb)	$\sigma_p(\frac{1}{4}E_\alpha)$ (mb)	$\sigma_\alpha/\sigma_p(E_\alpha)$	$\sigma_\alpha/\sigma_p(\frac{1}{4}E_\alpha)$
380	58.1 ^a	34 ^b	67 ^b	1.7	0.87
920	49.4 ^c	28.5 ^b	38.0 ^b	1.7	1.3

^aSee Ref. 5.

^bSee Ref. 6.

^cThis work.

and systematic errors were separately rms combined and then combined for the final-error estimate. The statistical and random errors of the mean are 2.1 and 3.0%. The total error is 3.7%. The cross section is 49.4 ± 1.8 mb.

COMPARISON WITH PREVIOUS WORK

Crandall *et al.*⁵ have measured $\sigma[C^{12}(x, xn)C^{11}]$, with $x = p, d, He^3$, and α ; and for 380-MeV α particles they find $\sigma = 58.1 \pm 1$ mb (after correcting 2% for gas loss from their ≤ 15 -mil polystyrene targets).¹³ Lindler and Osborn²² have measured $\sigma[C^{12}(\alpha, \alpha n)C^{11}]$ from threshold to 380 MeV and find $\sigma = 48.5 \pm 5$ mb at 380 MeV. A check exists on the Crandall *et al.* measurements, as their α cross section was measured in the same manner as their p cross section.²³ As the latter compares well with accepted values,⁶ the Crandall *et al.* value for the α cross section at 380 MeV is taken.

In Table II are tabulated E_α (kinetic energy of the α), σ_α , σ_p (at E_α), σ_p (at $\frac{1}{4}E_\alpha$, the same velocity as the α), and the ratio σ_α/σ_p for the two proton energies. The ratios of the two cross sections at the two energies are the same when using the proton energy equal to the total α kinetic energy (column 5) indicating that in this energy range the $C^{12}(x, xn)C^{11}$ cross section for different x appears to be dependent on the kinetic energy of x , not its velocity.

APPENDIX

Beam characteristics. There are two α beams in the 184-in. cyclotron of approximately equal intensity and energy.²⁴ During the preliminary

beam focusing work, we found it impossible to bring both beams down the beam pipe and not strike the pipe. Consequently, the premagnet collimator was closed down allowing only one beam to pass through the steering magnet. There was no collimation after the steering magnet. Preliminary beam focusing produced a beam which was uniform within $\pm 20\%$ over 5×5 cm and rapidly fell off to $< 0.5\%$ at 20 cm off beam center. During the course of the experiment, the range of the beam was repeatedly measured by the LRL Medical Physics group, who were operating under the same collimating and steering magnet conditions. Their range of 54-mm Cu to the Bragg peak and ~ 55 -mm Cu to the 50% beam reduction level, scaled by means of the proton range tables of Barkas and Berger,²⁵ gives a beam energy of 920 ± 20 MeV.

ACKNOWLEDGMENTS

A special note of appreciation is given to my advisor, Serge A. Korff, and to Rosalind Mendell for their patience and encouragement. Special thanks are given to Rein Silberberg for his extensive discussions with me at a meeting of the American Physical Society. Special thanks are given to LRL directors, Robert L. Thornton and Edwin M. McMillan, for providing free time on the cyclotron; to the entire Health Physics group at LRL, and in particular to Wade Patterson, Alan Smith, and Joseph McCaslin for putting their experimental area and instruments at my disposal and for their advice. Recognition is given to Arthur Poskanzer for his interest, excellent suggestions, and for his comments on the preliminary draft; to the Visual Measurements group at LRL, especially to Harry H. Heckman for his help in the initial cyclotron runs, to Thomas Coen for his continual aid in the emulsion processing, and to Dora Doughty for typing the manuscript; to Christine O'Connell for her excellent scanning; and to the 184-in. cyclotron crew for always providing an excellent beam. The help of all the members of the Cosmic Ray group at New York University is acknowledged. A last and special note of thanks to Arthur Feiner for his questions and analysis.

*Work supported in part by the National Aeronautics and Space Administration under Grant Nos. NGL-33-016-067 and NAS 1-5209, and by the Atomic Energy Commission.

¹D. V. Reames, in *High Energy Nuclear Reactions in Astrophysics*, edited by B. S. P. Shen (W. A. Benjamin Inc., New York, 1967).

²V. L. Ginzburg and S. I. Syrovatskii, in *The Origin of Cosmic Rays*, translated by H. S. W. Massey and edited

by D. ter Haar (Macmillan Company, New York, 1964).

³G. Alexander and G. Yekutieli, *Nuovo Cimento* **19**, 103 (1961).

⁴P. L. Jain, E. Lohrmann, and M. W. Teucher, *Phys. Rev.* **115**, 643 (1959).

⁵W. E. Crandall, G. P. Millburn, R. V. Pyle, and W. Birnbaum, *Phys. Rev.* **101**, 329 (1956).

⁶J. B. Cumming, *Ann. Rev. Nucl. Sci.* **13** (1963).

⁷R. G. Korteling and E. K. Hyde, *Phys. Rev.* **136**, B425 (1964).

⁸J. B. Cumming and R. Hoffman, *Rev. Sci. Instr.* **29**, 1104 (1958).

⁹A. M. Poskanzer, L. P. Remsberg, S. Katcoff, and J. B. Cumming, *Phys. Rev.* **133**, B1507 (1964).

¹⁰Pilot Chemical Company, 36 Pleasant Street, Watertown, Massachusetts.

¹¹Ilford Ltd., Ilford, Essex, England.

¹²Pilot Chemical Company, private communication.

¹³J. B. Cumming, A. M. Poskanzer, and J. Hudis, *Phys. Rev. Letters* **6**, 484 (1961).

¹⁴*Amperex Data Handbook* (Amperex Company, Hicksville, Long Island, New York, 1967).

¹⁵J. B. Cumming, G. Friedlander, and S. Katcoff, *Phys. Rev.* **125**, 2078 (1962).

¹⁶C. M. Lederer, J. M. Hollander, and I. Perlman, *Table of Isotopes* (John Wiley & Sons, Inc., New York, 1967), 6th ed.

¹⁷Jonathan Radin program (unpublished).

¹⁸The low value of χ^2 (deg freedom) is a consequence of an error in the weighting scheme wherein the high counting efficiency and long ($>\lambda$) counting times reduce the

standard deviation used here of (number of counts)^{1/2}, c.f., G. Friedlander, J. W. Kennedy, and J. M. Miller, *Nuclear and Radio-Chemistry* (John Wiley & Sons, Inc., New York, 1955), 2nd ed., p. 174ff. The error was not corrected.

¹⁹W. C. Davidon, Variable Metric Method of Minimalization, Argonne National Laboratory Report No. ANL-5990, 1959 (unpublished); E. Beals, University of California Lawrence Radiation Laboratory, program LSQVMT (unpublished).

²⁰Ilford Technical Information circular No. Y44.1 (unpublished).

²¹W. H. Barkas, *Nuclear Research Emulsions* (Academic Press, Inc., New York, 1963.).

²²M. Lindler and R. N. Osborn, *Phys. Rev.* **91**, 1501 (1953).

²³W. E. Crandall, private communication.

²⁴Lawrence Radiation Laboratory Medical Physics group, private communication.

²⁵W. H. Barkas and M. J. Berger, *Tables of Energy Losses and Ranges of Heavy Charged Particles*, The National Aeronautics and Space Administration Report No. NASA Sp-3013, 1964 (unpublished).

Nuclear Rotation: Cranking-Model Calculations and Their Relation to Other Treatments*

Chin W. Ma[†] and John O. Rasmussen

Heavy Ion Accelerator Laboratory, Yale University, New Haven, Connecticut 06520

(Received 27 January 1970)

The generalized cranking model is used to study the corrections to the nuclear rotational spectra that cause it to deviate from the $I(I+1)$ rule. The fourth-order cranking corrections and the Coriolis-antipairing effect are treated as modes of a generalized vibration in the same way as the centrifugal stretching. The new form helps to explain the success of various two-parameter formulas used to fit the experimental energy levels and shows that they are equivalent. The parameters of such formulas are calculated here microscopically in a good- j basis, and they agree reasonably well with experiment.

I. INTRODUCTION

In recent years the nuclear rotational problem has attracted considerable interest. One of the main reasons is that the development of the high-resolution solid-state γ detector made it possible to follow the rotational bands up as high as spin 18 (Stephens, Lark, Diamond).¹ The new results showed that the energies of the high-spin rotational states strongly deviate from the following well-known $I(I+1)$ rule of a rigid rotor:

$$E = I(I+1)/2\mathcal{J}, \quad (1.1)$$

where \mathcal{J} is called the moment of inertia. The trend is that \mathcal{J} increases with the angular momentum I of the level. A number of efforts have since been directed at understanding the deviations from the rigid rotor formula. There are two general ap-

proaches. One approach involves a microscopic calculation based usually on the second-order cranking model first suggested by Inglis²; corrections arise from taking into account the centrifugal stretching and the Coriolis-antipairing (CAP) effect suggested first by Mottelson and Valatin³ (Udagawa and Sheline⁴; Chan and Valatin⁵; Bes, Landowne, and Mariscotti⁶; Krumlinde⁷; and Marshalek⁸). Of these treatments Marshalek's is the only one carried out generally to fourth order. Others have tried to fit the energy levels by two-parameter formulas of various forms.⁹⁻¹⁵ Most of them can be derived either from the fourth-order cranking model (Harris)¹⁰ or from the centrifugal stretching model, namely,

$$E = \frac{1}{2}C_t(t-t_0)^2 + I(I+1)/2\mathcal{J}(t), \quad (1.2)$$

$$\partial E / \partial t = 0,$$